SUB6 Subtilisin is Involved During the Initial Adhesion of *Trichophyton benhamiae* and *T. mentagrophytes* onto Reconstructed Human Epidermis

Émilie Faway[1], Wilfried Poirier[2], Tsuyoshi Yamada[3,4], Kiyotaka Ozawa[3,5], Michel Monod[6], Bernard Mignon[2] and Yves Poumay[1]

JID Innovations (2025);**5:**100370 doi:10.1016/j.xjidi.2025.100370

The growing incidence of dermatophytoses and the emergence of strains resistant to available antifungal agents raise the need for a better understanding of the virulence mechanisms of dermatophytes to identify new therapeutic targets. The proteases of the subtilisin family have previously been highlighted as potential virulence factors for dermatophytes, in particular the protease SUB6, which was first discovered to be an allergen capable of inducing immediate and delayed hypersensitivity skin reactions. Moreover, *SUB6* expression and SUB6 protein production were detected during experimental and natural skin infections with several dermatophyte species. In this study, we specifically investigated the importance of SUB6 during *Trichophyton benhamiae* and *T. mentagrophytes* dermatophytosis in a reconstructed human epidermis model by comparing parental strains with genetically engineered ones deleted (Δ*SUB6*) or complemented for the SUB6-encoding gene. Thereby, a role for SUB6 has been identified in the initial steps of adhesion to the host epidermal surface. However, the Δ*SUB6* strains were able to finally invade the reconstructed human epidermis, suggesting that SUB6 is a robust fungal marker of infection but not an essential virulence factor.

Keywords: Adhesion, Dermatophytosis, Reconstructed human epidermis, Subtilisin, Virulence factor

INTRODUCTION

Dermatophytoses are the most common mycoses worldwide, with a prevalence of 20–25% (Havlickova et al, 2008; Zhan and Liu, 2017). The incidence is much more elevated in some geographical areas, such as in India, where an epidemic-like scenario of dermatophytosis is occurring (Verma et al, 2021). Of concern is the current emergence of strains resistant to usual antifungal drugs (Gupta et al, 2024; Monod et al, 2023; Sacheli and Hayette, 2021), particularly related to the limited antifungal therapeutic targets identified to date. Dermatophytoses therefore represent a burden for public health, and there is a current need for a better understanding of their pathogenesis, especially to identify new targets for the development of innovative treatments.

Subtilisin proteases belong to a family comprising 12 members, named SUB1–12, and were highlighted as potential virulence factors of dermatophytes (Gräser et al, 2018; Monod, 2008; Satala et al, 2023; Vermout et al, 2008). Although members of the subtilisin family are generally involved in the degradation of infected keratinized structures, some may exert specific roles. For instance, a role for SUB3 in the adhesion of *Microsporum canis* spores to the host epidermis was demonstrated using *in vitro* and *ex vivo* models (Băguţ et al, 2012; Baldo et al, 2010, 2008). However, important variations in fungal expression profiles analyzed during *in vivo* infection or during growth *in vitro* on synthetic agar, especially regarding expression of subtilisin-encoding genes, suggest that dermatophytes can evolve under 2 distinct phenotypes: a saprophytic one and an infectious one (Staib et al, 2010; Tran et al, 2016). In particular, although *SUB3* and *SUB4* genes appear highly expressed by *Trichophyton benhamiae* during *in vitro* growth on keratin-enriched agar, there is little or no expression while this species is infecting its natural host guinea pigs *in vivo* (Staib et al, 2010; Tran et al, 2016).

Of particular interest, whereas the *T. rubrum* SUB6 protease was initially reported as a major allergen capable of inducing immediate and delayed hypersensitivity skin reactions in

[1]*Molecular Physiology Research Unit, NAmur Research Institute for Life Sciences (URPHYMNARILIS), Faculty of Medicine, University of Namur, Namur, Belgium;* [2]*Fundamental and Applied Research for Animals & Health (FARAH), Faculty of Veterinary Medicine, University of Liège, Liège, Belgium;* [3]*Teikyo University Institute of Medical Mycology, Teikyo University, Tokyo, Japan;* [4]*Asia International Institute of Infectious Disease Control, Teikyo University, Tokyo, Japan;* [5]*Medical Mycology Research Center, Chiba University, Chiba, Japan; and* [6]*Department of Dermatology, Centre Hospitalier Universitaire Vaudois, Lausanne, Switzerland*

Correspondence: Emilie Faway, Molecular Physiology Research Unit, NAmur Research Institute for Life Sciences (URPHYM-NARILIS), University of Namur, Namur 5000, Belgium. E-mail: emilie.faway@unamur.be

Abbreviations: RHE, reconstructed human epidermis; SGA, Sabouraud glucose agar; TEER, transepithelial electrical resistance; UTR, untranslated region; WT, wild-type

Received 25 October 2024; revised 1 March 2025; accepted 24 March 2025; accepted manuscript published online 11 April 2025; corrected proof published online 3 May 2025

Cite this article as: JID Innovations 2025;5:100370

humans (Woodfolk et al, 1998), the *SUB6* gene appeared as the second most highly expressed gene by *T. benhamiae* during infection in guinea pigs (Staib et al, 2010; Tran et al, 2016). In addition, the SUB6 protease was detected in humans with *T. rubrum* onychomycosis (Méhul et al, 2016) and in *T. verrucosum* bovine ringworm (Lindenhahn et al, 2021). Those observations altogether suggest that SUB6 is a relevant marker of dermatophytosis that could simultaneously play important roles in the infectious process during dermatophytosis.

In this study, the role played by SUB6 during infection was investigated through models of *T. benhamiae* and *T. mentagrophytes* dermatophytosis in reconstructed human epidermis (RHE). This model efficiently recapitulates the infection mechanisms deployed by *T. benhamiae* during infection of its natural hosts, including a strong expression of *SUB6* (Faway et al, 2025). Infection of RHE by *SUB6* gene—deleted strains of *T. benhamiae* and *T. mentagrophytes* was analyzed and revealed the involvement of SUB6 during the initial steps of adhesion but no further impairment of host tissue invasion by deleted strains. Results suggest that SUB6 is a robust fungal marker of infection, the presence of this protease being associated with the infectious phenotype of dermatophytes, but is not an essential virulence factor required for the development of infection.

RESULTS

SUB6-deleted strains of *T. benhamiae* quickly invade the human epidermis despite weaker initial adhesion

The *T. benhamiae KU70*—lacking mutant (Tb-Δ*KU70*), derived from the wild-type (WT) IHEM 20161 strain (ie, Tb-WT), was used as the recipient strain to generate a *SUB6*-deleted strain (Tb-Δ*SUB6*) and a *SUB6*-complemented strain (Tb-*SUB6*c), as described in the Materials and Methods section (Table 1). Each strain of *T. benhamiae* was tested for RHE infection following a procedure developed by Faway et al (2019, 2017). As previously observed with the Tb-WT strain (Faway et al, 2025), the invasion of the epidermis by the Tb-Δ*KU70*, Tb-Δ*SUB6*, and Tb-*SUB6*c strains progressed over time, reaching full thickness after 4 days of infection, with no difference between strains, suggesting that SUB6 is dispensable for the invasion to occur (Figure 1a). To mimic *in vivo* lesions restricted to the cornified layer, *T. benhamiae* infection in RHE was always analyzed on day 3 after infection, when hyphae remain localized superficially in the epidermis.

Histological analysis of infected RHE recovered on day 3 after infection showed a deeper invasion for the Tb-Δ*SUB6* strain than for the other *T. benhamiae* strains, which was confirmed by measuring the extent of invasion (Figure 1a and b). In parallel, transepithelial electrical resistance (TEER) measurements through infected RHE revealed that the Tb-Δ*SUB6* strain more rapidly altered the epidermal barrier integrity than any other strain (Figure 1c). Surprisingly, the Tb-Δ*SUB6* strain was also characterized by a slower initial adhesion to the epidermal surface, measured during the first 2 hours after inoculation (Figure 1d). Notably, after 4 hours of contact, the adhesion of the Tb-Δ*SUB6* strain reached a level identical to that observed with all other strains (Figure 1d).

Deletion of *SUB6* also impairs the initial adhesion in *T. mentagrophytes*

The *T. mentagrophytes KU80*—lacking mutant (Tm-Δ*KU80*), derived from the WT TIMM 2789 (Tm-WT) strain, was used as the recipient strain to generate an *SUB6*-deleted strain (Tm-Δ*SUB6*) and an *SUB6*-complemented strain (Tm-*SUB6*c), as described in the Materials and Methods section (Table 2). After RHE infection with WT and mutant strains of *T. mentagrophytes*, the fungal invasion progressed similarly over time and remained in the cornified layer within the first 4 days after infection (Figure 2a), allowing analysis of *T. mentagrophytes* infection in RHE on day 4 after infection and suggesting that SUB6 is not critical for invasion (Figure 2a and b). TEER measurements through infected RHE showed that the integrity of the epidermal barrier was altered as early as on day 2 after infection and more significantly during infection with the Tm-Δ*SUB6* strain than with others (Figure 2c). Interestingly and consistent with what was observed with *T. benhamiae*, reduced adhesion to the epidermal surface was observed 30 minutes after RHE inoculation with the Tm-Δ*SUB6* strain (Figure 2d).

Early and late infection time points refer to adhesion and invasion steps

On the basis of adhesion and invasion kinetics, 2 time points were determined to study the mechanisms of infection: one for "early infection" and one for "late infection." In practice, the early infection time point corresponds to the duration of contact between spores and RHE from which the adhesion of the WT strain reaches at least 25%, which is 30 minutes for both *T. benhamiae* and *T. mentagrophytes* (Figures 1d and 2d). The late infection time point is when the invasion by the WT strain is sufficiently developed but still restricted to the superficial layers of the epidermis, which happens on day 3 after infection for *T. benhamiae* and on day 4 after infection for *T. mentagrophytes* (Figures 1a and 2a).

It is important to note that RHE represents a suitable model to induce the infectious phenotype in *T. benhamiae* because 3 fungal genes previously suggested as markers of

Table 1. Strains of *Trichophyton benhamiae* Used in this Study

Name of the Strain	Abbreviation	Identification Number	Genotype
WT strain	Tb-WT	IHEM 20161	—
Recipient strain	Tb-Δ*KU70*	ΔTbeKu70-5-1 (TIMM40015; IFM 66349)[1]	*KU70*-lacking mutant
SUB6-deleted strain	Tb-Δ*SUB6*	ΔAbSUB6-14-5	*KU70*-lacking and *SUB6*-lacking mutant
SUB6-complemented strain	Tb-*SUB6*c	AbSUB6C-23-3	*KU70*-lacking and *SUB6*-lacking mutant, reintroduction of the *SUB6* gene

Abbreviation: WT, wild-type.
[1]Yamada et al (2021).

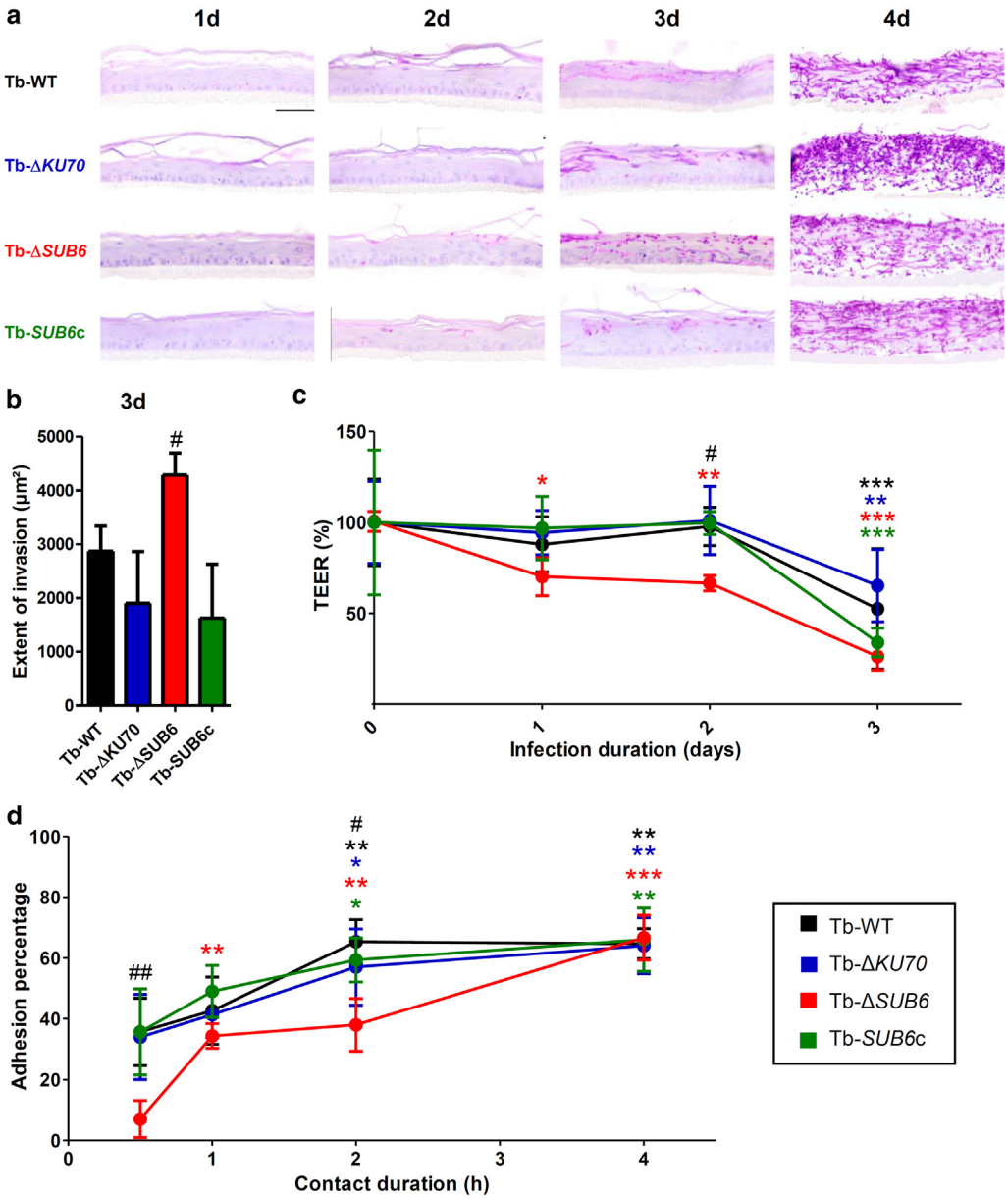

Figure 1. Development of the infection with the deleted strains of *Trichophyton benhamiae* on RHE. (**a**) RHE was infected with the WT (Tb-WT), recipient (Tb-Δ*KU70*), deleted for *SUB6* (Tb-Δ*SUB6*), and complemented for *SUB6* (Tb-*SUB6*c) strains of *T. benhamiae* and recovered daily during the 4 days after infection (1d to 4d) for histological processing and Periodic-acid Schiff staining with α-amylase pretreatment and hemalun counterstaining (bar = 50 µm). **(b)** The area occupied by fungal elements on day 3 after infection (3d) was quantified on histological slides (n = 3, mean + SD; 1-way ANOVA; $^{\#}P < .05$ showing statistical differences between the Tb-Δ*SUB6* strain and the other strains). **(c)** TEER was measured daily during infection to assess the epidermal barrier integrity. TEER values are expressed as a percentage of the values measured before infection (0 days; n = 3, mean ± SD; 2-way repeated-measures ANOVA; $^{*}P < .05$, $^{**}P < .01$, and $^{***}P < .001$ indicate statistical differences for each strain compared with 0 days; $^{\#}P < .05$ indicates statistical differences between the Tb-Δ*SUB6* strain and the other strains at each time point). **(d)** The adhesion percentage of *T. benhamiae* to epidermis was determined after different contact durations, from 0.5 to 4 h (n = 3, mean ± SD; 2-way ANOVA; $^{*}P < .05$, $^{**}P < .01$, and $^{***}P < .001$ indicate statistical differences for each strain compared with 0.5 h; $^{\#}P < .05$ and $^{\#\#}P < .01$ indicate statistical differences between the Tb-Δ*SUB6* strain and the other strains at each time point). h, hour; RHE, reconstructed human epidermis; TEER, transepithelial electrical resistance; WT, wild-type.

dermatophytosis infection, namely naphthalene reductase (*ARP2*), a deuterolysin (*DEUT*), and thaumatin (*THAU*), were overexpressed during RHE infection (Faway et al, 2025; Tran et al, 2016). In this study, similar data are reported on day 4 after infection during *T. mentagrophytes* infection in RHE, demonstrating that RHE is again a suitable model to analyze the infectious phenotype of *T. mentagrophytes* (Figure 2e and f).

Similar inflammatory responses are induced in RHE during infection by the deleted and parental strains of *T. benhamiae* and *T. mentagrophytes*

The establishment of an inflammatory response by the host during RHE infection with the mutant strains of *T. benhamiae* and *T. mentagrophytes* was assessed by measuring the mRNA expression of the proinflammatory cytokines *IL1β* and *TNFα* and the antimicrobial peptide *BD2* (β-defensin-2)

Table 2. Strains of *Trichophyton mentagrophytes* Used in this Study

Name of the Strain	Abbreviation	Identification Number	Genotype
WT strain	Tm-WT	TIMM 2789[1]	—
Recipient strain	Tm-Δ*KU80*	1062Av1401[2]	*KU80*-lacking mutant
SUB6-deleted strain	Tm-Δ*SUB6*	Av1101-6-7-4[2]	*KU80*-lacking and *SUB6*-lacking mutant
SUB6-complemented strain	Tm-*SUB6*c	Av1101-6C-1-9	*KU80*-lacking and *SUB6*-lacking mutant, reintroduction of the *SUB6* gene

Abbreviation: WT, wild-type.
[1]Uchida et al (2003).
[2]Yamada et al (2014).

by RT-qPCR after total RNA extraction (Figure 3). All these inflammatory markers were similarly overexpressed at the late infection time point, regardless of the mutant strain used for *T. benhamiae* and *T. mentagrophytes*. It should be noted that no overexpression of proinflammatory markers can be detected during early infection (Faway et al, 2025), likely because contact between fungal elements and subcorneal living keratinocytes is required to induce keratinocyte responses (Faway et al, 2019).

SUB9* is overexpressed in the absence of *SUB6

Fungal subtilisin mRNA expression was assessed by RT-qPCR during RHE early and late infection with *T. benhamiae* and *T. mentagrophytes*. For both species, few differences in fungal gene expression were observed between the recipient and the WT strains ($P = .044$ for *SUB1* relative mRNA expression measured at late infection between Tb-Δ*KU70* and Tb-WT and $P = .024$ for *SUB11* relative mRNA expression measured at early infection between Tm-Δ*KU80* and Tm-WT) (Figure 4), suggesting that the deletion of the *KU70* or *KU80* gene or the process of genetic manipulation only slightly affects the fungal phenotype of *T. benhamiae* or *T. mentagrophytes*. To account for this small effect of genetic manipulation, the fungal subtilisin mRNA expression levels in the Δ*SUB6* and *SUB6*c strains were compared with those in corresponding recipient strains.

For *T. benhamiae*, a rather different expression profile was observed between early and late infection time points, suggesting that distinct mechanisms are involved in *T. benhamiae* adhesion and invasion (Figure 5a and b). Indeed, although the *SUB6* and *SUB10* genes were already overexpressed by *T. benhamiae* during early infection, overexpression of the *SUB1* gene was only observed during late infection. Overall, all mutant strains of *T. benhamiae* showed the same expression profile, except for the *SUB9* gene, which was only overexpressed by the Tb-Δ*SUB6* strain during late infection ($P = .016$ and $P = .002$ in comparison with Tb-Δ*KU70* strain and Tb-*SUB6*c strain, respectively). As expected, no expression of the *SUB6* gene could be detected in the Tb-Δ*SUB6* strain.

For *T. mentagrophytes*, little expression of subtilisin genes was measured during early infection, regardless of the strain used (Figure 5c). However, it is important to note that for *SUB6* and *SUB10* genes, the basal expression in *T. mentagrophytes* spores, collected after growth in potato dextrose agar, is quite high compared with that in *T. benhamiae* spores, suggesting an elevated basal expression for these 2 genes in *T. mentagrophytes* spores (Figure 6). During late infection, *T. mentagrophytes* overexpressed several subtilisin genes: *SUB1*, *SUB3*, *SUB4*, *SUB5*, *SUB6*, *SUB8*, *SUB9*, and *SUB10* (Figure 5d). Interestingly, as already observed for *T. benhamiae*, *SUB9* appeared to be more highly expressed by the Tm-Δ*SUB6* strain than by the others, although this difference was not statistically significant ($P = .091$ and $P = .068$ in comparison with Tm-Δ*KU80* strain and Tm-*SUB6*c strain, respectively).

DISCUSSION

Despite the growing global incidence of dermatophytoses, a very limited number of studies have investigated the fungal virulence mechanisms underlying the initiation and development of such superficial infections. Members of the subtilisin protease family have long been evoked as potential virulence factors for dermatophytes (Gräser et al, 2018; Monod, 2008; Satala et al, 2023; Vermout et al, 2008). Interestingly, *SUB6* was found to be the most overexpressed secreted protease-encoding gene by *T. benhamiae* during the experimental infection in guinea pigs, its natural host (Staib et al, 2010; Tran et al, 2016), suggesting that SUB6 may play an active role in the development of infection. Deleted and complemented strains of dermatophytes have already been successfully used to unravel the role of a specific gene in the pathogenic phenotype of dermatophytes (Ishii et al, 2023). This study successfully generated Δ*SUB6* and *SUB6*c strains of *T. benhamiae* and *T. mentagrophytes* from the parental strains Δ*KU70* and Δ*KU80*, respectively. Then, through infection on RHE using these genetically engineered strains, we specifically investigated the role of SUB6 during *T. benhamiae* and *T. mentagrophytes* infections.

Because transcriptomic studies have shown that *T. benhamiae* expresses a different set of genes when growing on synthetic agar or during *in vivo* infection (Staib et al, 2010; Tran et al, 2016), it seems crucial to use an adequate model for dermatophytosis. As previously shown for *T. rubrum* and *T. benhamiae* (Faway et al, 2025), in this study, we demonstrate overexpression of 3 fungal genes previously identified as infection markers (ie, *ARP2*, *DEUT*, and *THAU*) during RHE infection by *T. mentagrophytes*, confirming that the dermatophytosis model on RHE recapitulates the infectious phenotype of dermatophytes. Despite some intrinsic limitations (Faway et al, 2021b), the RHE model therefore appears as a valuable tool to study the pathogenesis of dermatophytosis. Especially, the RHE model enables the analysis of the

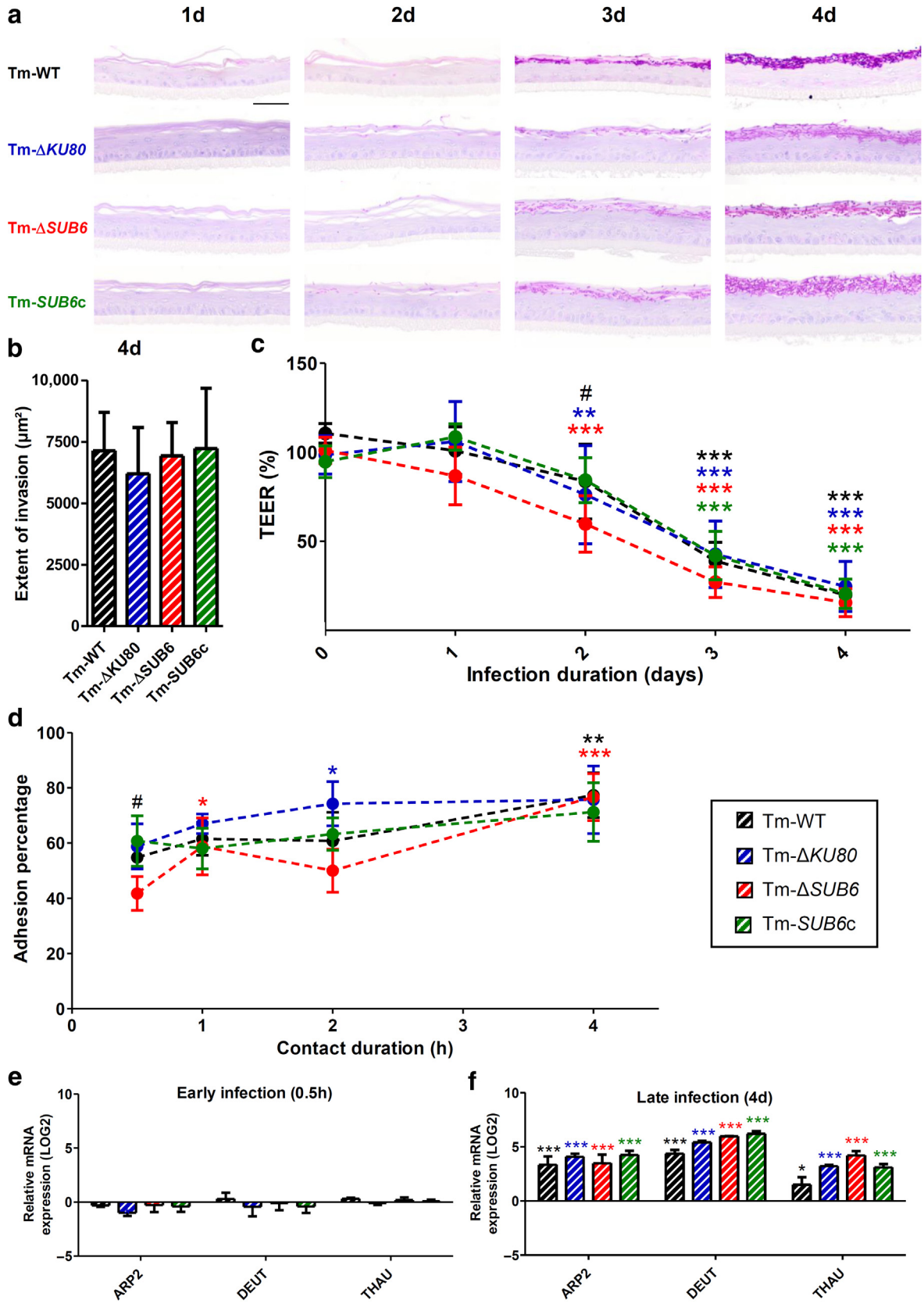

Figure 2. Development of the infection with the deleted strains of *Trichophyton mentagrophytes* on RHE. (**a**) RHE was infected with the WT (Tm-WT), recipient (Tm-Δ*KU80*), deleted for *SUB6* (Tm-Δ*SUB6*), and complemented for *SUB6* (Tm-*SUB6*c) strains of *T. mentagrophytes* and recovered daily during the 4 days after infection (1d to 4d) for histological processing and Periodic-acid Schiff staining with α-amylase pretreatment and hemalun counterstaining (bar = 50 µm). **(b)** The area occupied by fungal elements on day 4 after infection (4d) was quantified on histological slides (n = 3, mean + SD; 1-way ANOVA; $P > .05$). **(c)** TEER was measured daily during infection to assess the epidermal barrier integrity. TEER values are expressed as a percentage of the values measured before infection

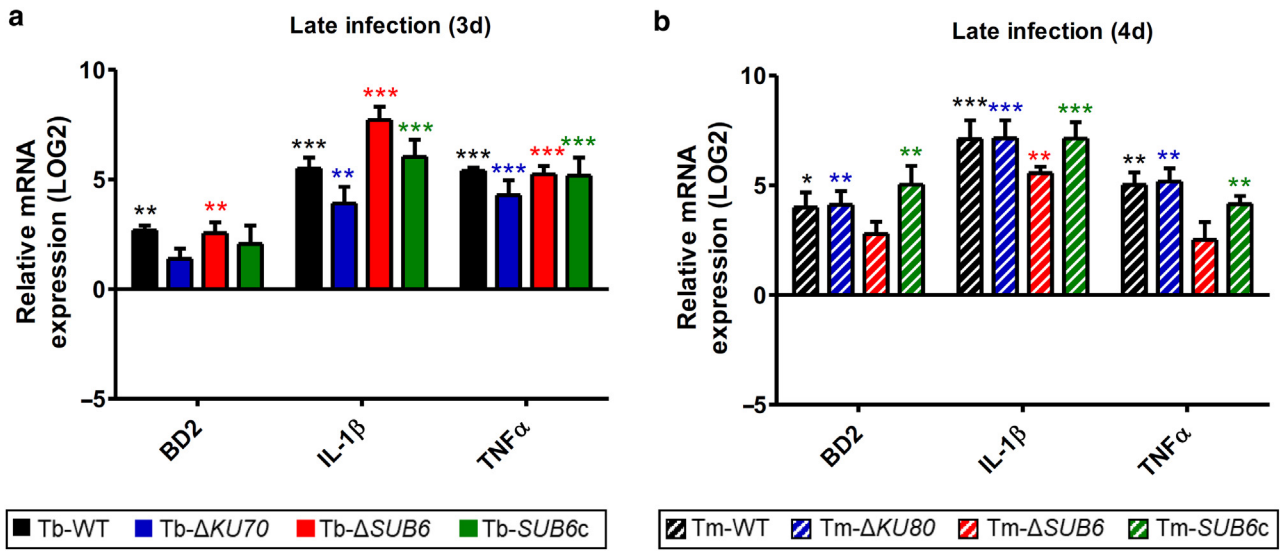

Figure 3. Host inflammatory responses during dermatophyte infection on RHE. Relative mRNA expression of host proinflammatory cytokines (*IL1β* and *TNFα*) and antimicrobial peptides (*BD2*) was assessed by RT-qPCR after total RNA extraction from RHE infected with WT, recipient (Δ*KU70* or Δ*KU80*), deleted for *SUB6* (Δ*SUB6*), and complemented for *SUB6* (*SUB6*c) strains of **(a)** *Trichophyton benhamiae* (denoted as Tb) and **(b)** *T. mentagrophytes* (denoted as Tm) and collected **(a)** 3 (3d) or **(b)** 4 (4d) days after infection. The mRNA expression level is calculated relative to the expression level measured in uninfected control RHE (n = 3, mean + SD; 2-way ANOVA; **P* < .05, ***P* < .01, and ****P* < .001 indicate statistically significant differences for each strain compared with expression in control; no statistically significant difference was observed between strains). Complete names and accession numbers of studied genes are listed in Supplementary Table S3. BD2, β-defensin-2; RHE, reconstructed human epidermis; WT, wild-type.

early fungal stages of infection, namely adhesion and germination (Faway et al, 2021b, 2017; Tirtiaux et al, 2025).

Interestingly, as previously shown for *T. benhamiae* during infection in RHE and mouse model and for *T. rubrum* during RHE infection (Faway et al, 2025), a strong expression of *SUB6* is also detected during *T. mentagrophytes* infection on RHE. Together with previous studies that successfully detected the protease SUB6 in guinea pig skin explants infected *ex vivo* with *T. benhamiae* (Baumbach et al, 2020) as well as in *T. rubrum* human onychomycosis (Méhul et al, 2016) and in *T. verrucosum* bovine ringworm (Lindenhahn et al, 2021), our observations suggest that the presence of this protease is associated with dermatophyte infection, regardless of the role SUB6 may or may not play in the infectious process. This reinforces the idea that SUB6 may be a robust marker of dermatophytosis, irrespective of the fungal species involved, and therefore represents an interesting diagnostic target. New diagnostic strategies based on the detection of SUB6 protease or encoding RNA may emerge for both human and veterinary medicine. These strategies should be faster than culture-based diagnosis and, in contrast to current DNA-based molecular diagnosis (Aho-Laukkanen et al, 2024), enable discrimination between infectious and dormant dermatophytes sometimes present in healthy carriers (Ilkit and Demirhindi, 2008). The Δ*SUB6* strains of *T. benhamiae* and *T. mentagrophytes* adhered less efficiently to the epidermal surface of RHE after 30 minutes and 2 hours of contact than the reference strains (Δ*KU70/80* and *SUB6*c), suggesting a role for SUB6 in the initial steps of adhesion. The fact that the same observation was made in 2 different *Trichophyton* species suggests that the involvement of SUB6 in adhesion may be conserved among dermatophyte species. Such a hypothesis is supported by the detection of SUB6 protease during natural infection with *T. rubrum* and *T. verrucosum* (Lindenhahn et al, 2021; Méhul et al, 2016). Although another subtilisin, SUB3, has previously been identified as involved in the adhesion of *M. canis* spores (Băguț et al, 2012; Baldo et al, 2010, 2008), the exact mechanism through which subtilisin proteases could participate in adhesion is not yet identified. It is neither clear whether the subtilisin proteases could be direct ligands for binding host structures or whether they proteolytically model other surface molecules on fungal or host cells. The involvement of a fungal protease in adhesion has already been demonstrated in *Aspergillus fumigatus*, whose alkaline protease 1 (Alp1/Asp f 13/oryzin) has been identified as a fibrinogen-binding protein, participating in the interactions of this fungus with the human extracellular matrix (Upadhyay et al, 2012).

(0 days; n = 3, mean ± SD; 2-way repeated-measures ANOVA; ***P* < .01 and ****P* < .001 indicate statistically significant differences for each strain compared with 0 days; $^{\#}P$ < .05 indicates statistical differences between the Tm-Δ*SUB6* strain and the other strains at each time point). **(d)** The adhesion percentage of *T. mentagrophytes* to epidermis was determined after different contact durations, from 0.5 to 4 h (n = 3, mean ± SD; 2-way ANOVA; **P* < .05, ***P* < .01, and ****P* < .001 indicate statistically significant differences for each strain compared with 0.5 h; $^{\#}P$ < .05 indicates statistically significant differences between the Tm-Δ*SUB6* strain and the other strains at each time point). **(e, f)** Relative mRNA expression of fungal marker genes was assessed by RT-qPCR during **(e)** early infection and **(f)** late infection. The mRNA expression level is calculated relative to the expression level measured in **(e)** nonactivated spores or **(f)** mycelium as control (n = 3, mean + SD; 2-way ANOVA; **P* < .05 and ****P* < .001 indicate differences compared with control for each strain; no statistically significant difference was observed between strains). Complete names and accession numbers of studied genes are listed in Supplementary Table S5. h, hour; RHE, reconstructed human epidermis; TEER, transepithelial electrical resistance; WT, wild-type.

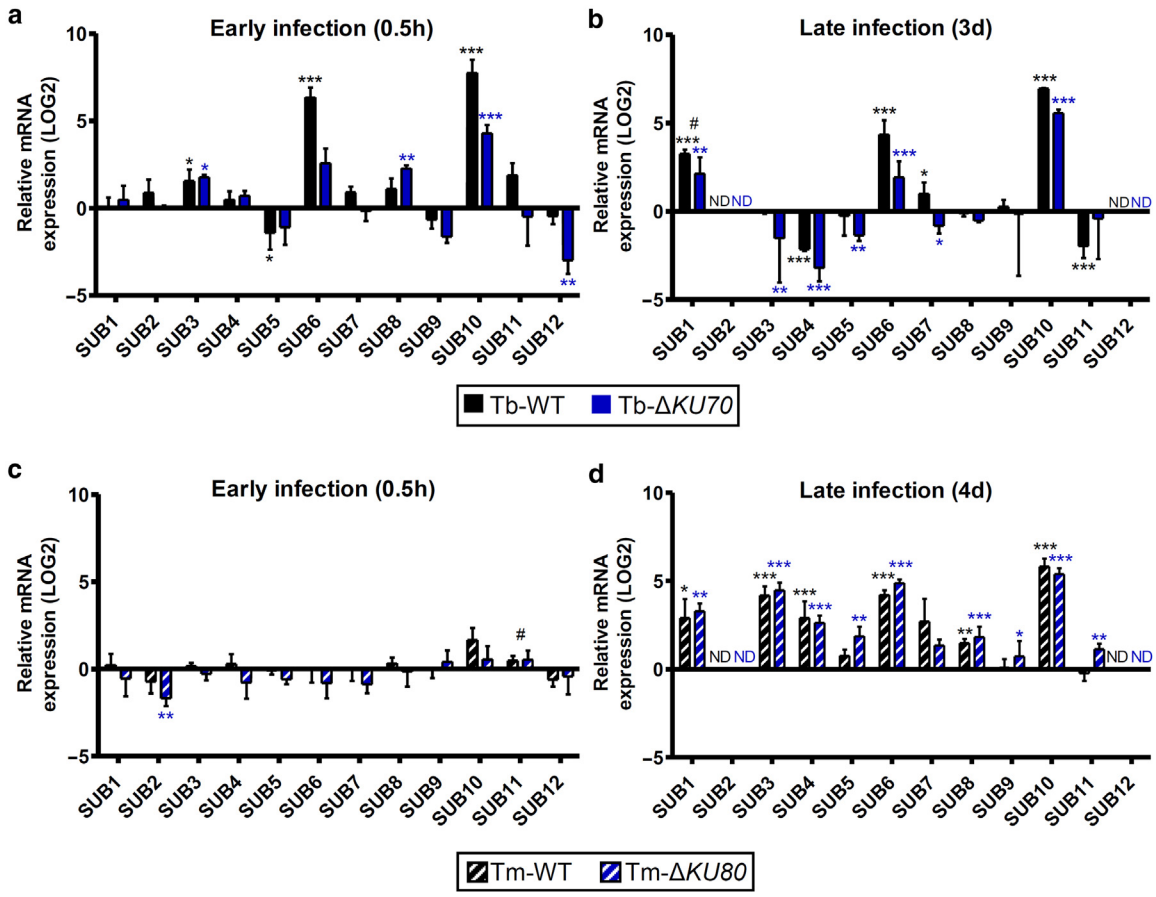

Figure 4. Fungal subtilisin expression by WT and parental strains of *Trichophyton benhamiae* and *T. mentagrophytes* during infection on RHE. Relative mRNA expression of fungal subtilisins was assessed by RT-qPCR during RHE **(a, c)** early and **(b, d)** late infection with the WT and recipient (Δ*KU70* and Δ*KU80*) strains of **(a, b)** *T. benhamiae* (denoted as Tb) and **(c, d)** *T. mentagrophytes* (denoted as Tm). The mRNA expression level is calculated relative to the expression level measured in **(a, c)** nonactivated spores or **(b, d)** mycelium as control (n = 3, mean + SD; 2-way ANOVA; $^{*}P < .05$, $^{**}P < .01$, and $^{***}P < .001$ indicate statistically significant differences compared with control for each strain; $^{\#}P < .05$ indicates statistically significant differences between WT and recipient strains for each gene; Cq > 45). Complete names and accession numbers of studied genes are listed in Supplementary Tables S4 and S5. h, hour; ND, nondetected; RHE, reconstructed human epidermis; WT, wild-type.

Furthermore, it could be hypothesized that the proteolytic activity of SUB6 may induce damage and cell death in host keratinocytes, thereby releasing intracellular motifs and impairing host defenses, which could finally facilitate adhesion and invasion.

Despite a potential role for SUB6 in the adhesion step, both *T. benhamiae* and *T. mentagrophytes* Δ*SUB6* strains were ultimately able to adhere to the host epidermis and invade the cornified layer of RHE. The *T. benhamiae* Δ*SUB6* strain appeared even more invasive than the reference strains, with a deeper level of invasion and some quicker alteration of the epidermal barrier integrity. A trend toward an accelerated impact on the epidermal barrier integrity was also observed for *T. mentagrophytes* Δ*SUB6* strain during RHE infection. These observations contrast with the findings of a previous study that had reported reduced virulence for a *SUB6*-deleted strain generated from *T. mentagrophytes* ATCC 28185 during experimental infection in guinea pigs (Shi et al, 2016). Because this ATCC 28185 strain has since then been reclassified as the anthropophilic species *T. interdigitale* (Suh et al, 2018), differences between the 2 studies may be due to the existence of distinct pathogenic mechanisms deployed by zoophilic (ie, *T. benhamiae* and *T. mentagrophytes*) and anthropophilic dermatophytes, as previously suggested (Faway et al, 2025). The invasion of RHE by the Δ*SUB6* strains of *T. benhamiae* and *T. mentagrophytes* strains suggests that SUB6 is definitely dispensable for adhesion and invasion to occur, most likely due to some compensatory mechanisms that appear in the absence of SUB6. Compensatory mechanisms between dermatophyte proteases have been previously reported during the infection in guinea pigs with the *SUB6*-deleted strain of *T. interdigitale* ATCC 28185, which overexpressed *SUB3* and *MEP4*, a metalloprotease-encoding gene, in comparison with the WT strain (Shi et al, 2016). During RHE infection, *SUB9* appeared to be significantly overexpressed by the Δ*SUB6* strain of *T. benhamiae*, and a similar trend was observed for *T. mentagrophytes*. Interestingly, although not statistically significant, a tendency toward higher expression of *SUB9* by the *ΔSUB6* strain of *T. benhamiae* was also observed during experimental infection in a mouse model (Poirier et al, 2025). In this mouse model, no difference was observed in clinical scores, tissular fungal invasion, or host inflammation induced by infection with reference and *ΔSUB6* strains of *T. benhamiae*. However, the

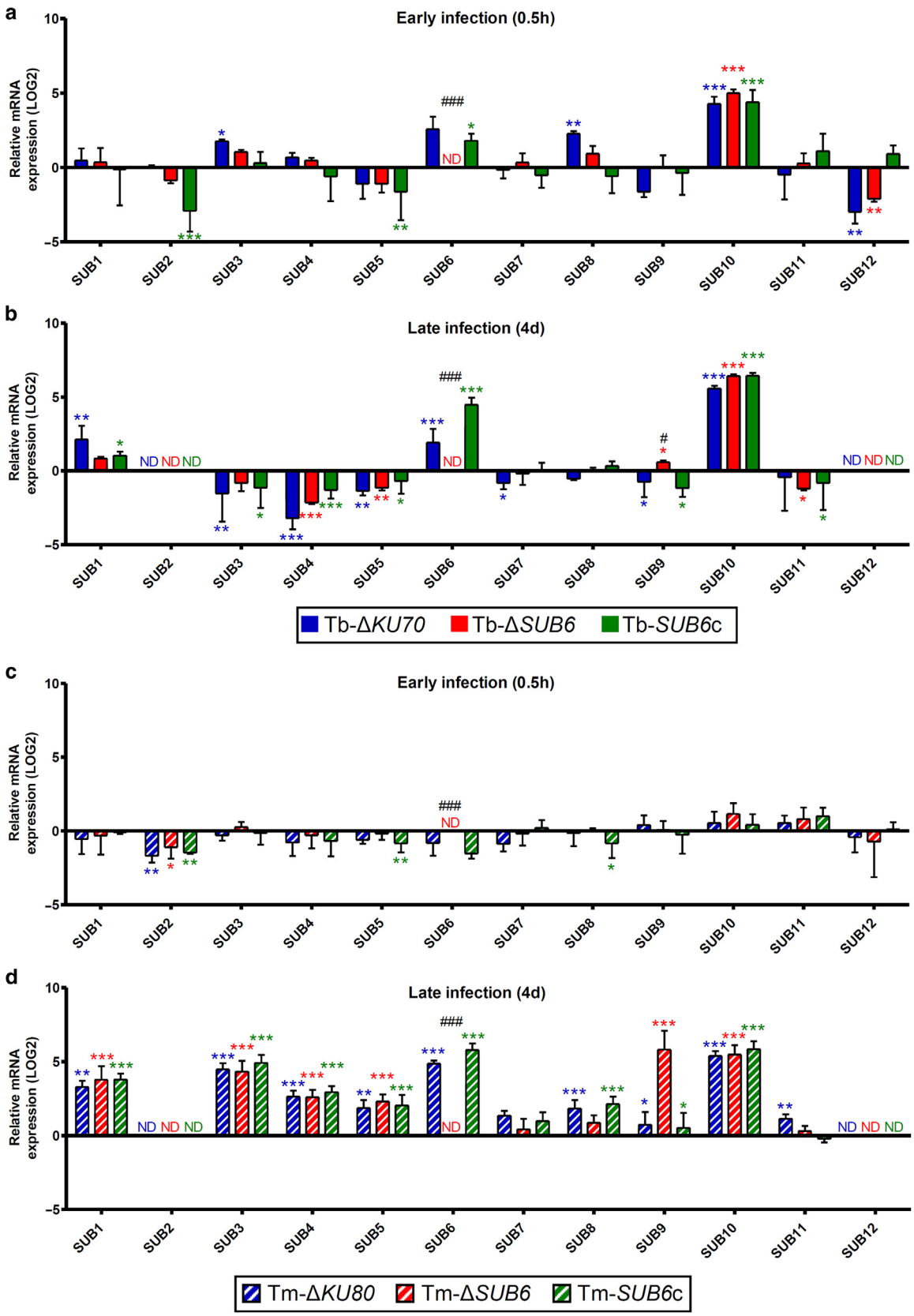

Figure 5. Fungal subtilisin expression by *Trichophyton benhamiae* and *T. mentagrophytes* during infection on RHE. Relative mRNA expression of fungal subtilisins was assessed by RT-qPCR during RHE **(a, c)** early infection and **(b, d)** late infection with recipient (Δ*KU70* or Δ*KU80*), deleted for *SUB6* (Δ*SUB6*), and complemented for *SUB6* (*SUB6*c) strains of **(a, b)** *T. benhamiae* (denoted as Tb) and **(c, d)** *T. mentagrophytes* (denoted as Tm). The mRNA expression level is calculated relative to the expression level measured in **(a, c)** nonactivated spores or **(b, d)** mycelium as control (n = 3, mean + SD; 2-way ANOVA; $^{*}P < .05$, $^{**}P < .01$, and $^{***}P < .001$ indicate statistically significant differences compared with control for each strain; $^{\#}P < .05$ and $^{\#\#\#}P < .001$ indicate statistically

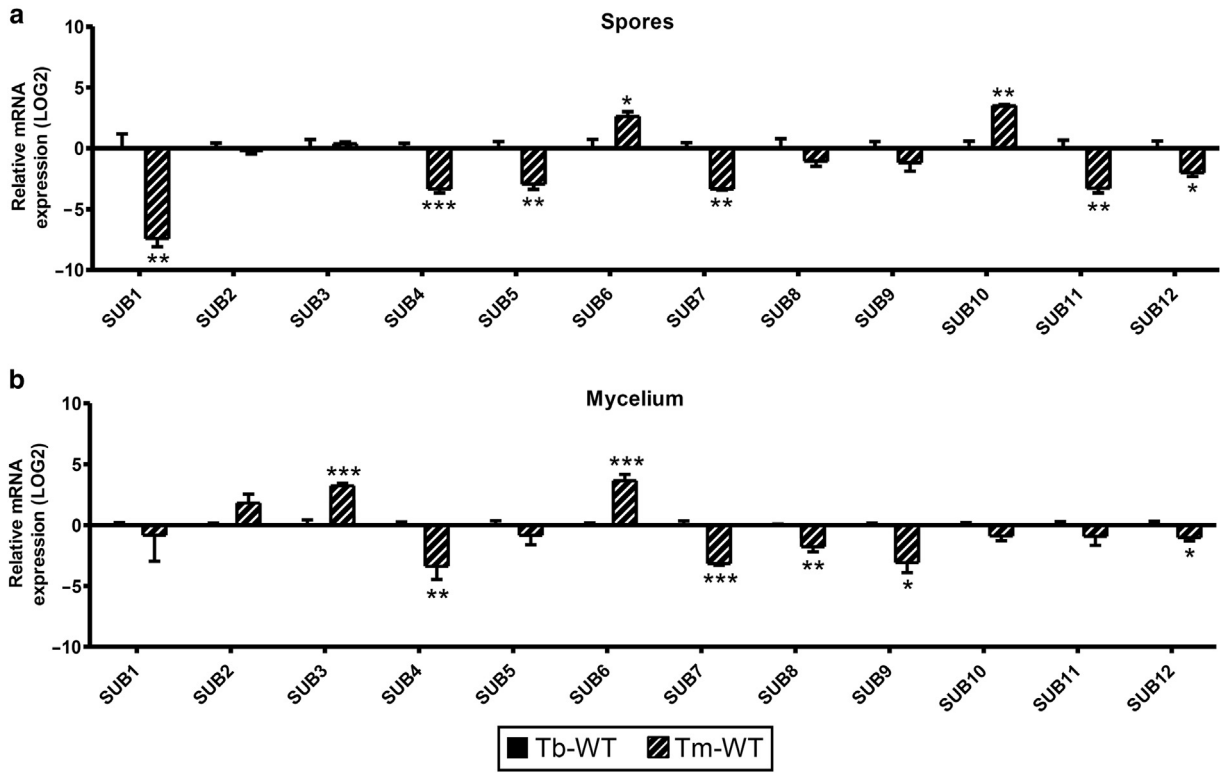

Figure 6. Basal expression of fungal subtilisins in spores and mycelium of *Trichophyton benhamiae* and *T. mentagrophytes*. Relative mRNA expression of fungal subtilisins was assessed by RT-qPCR after total RNA extraction from **(a)** a pellet of spores (collected after culture on potato dextrose agar) or **(b)** mycelium (recovered after 24 h of growth in Sabouraud glucose broth) of *T. benhamiae* (denoted as Tb) and *T. mentagrophytes* (denoted as Tm) WT strains. The relative expression level of each subtilisin for *T. mentagrophytes* is calculated relative to the expression for *T. benhamiae* (n = 3, mean + SD; 1-way ANOVA; $*P < .05$, $**P < .01$, and $***P < .001$ indicate statistically significant differences between *T. benhamiae* and *T. mentagrophytes* for each gene). Complete names and accession numbers of studied genes are listed in Supplementary Tables S4 and S5. h, hour; WT, wild-type.

mouse model does not allow the analysis of the early stages of infection, thus missing a potential effect on the adhesion step. Together, observations in RHE and mouse models suggest that *SUB9* expression might be involved in the compensatory mechanisms employed by dermatophytes lacking *SUB6*. The generation of strains deleted for *SUB9* as well as of multiple deleted strains for *SUB6* and *SUB9* and the subsequent infection in RHE and mouse models will allow to better characterize the respective roles of both these proteases. On the other hand, besides the subtilisin family, the involvement of other genes cannot be excluded. An RNA-sequencing analysis will therefore be performed to identify genes that are overexpressed during infection in the absence of *SUB6*. Furthermore, these compensatory mechanisms, probably involving the upregulation of other proteases such as *SUB9*, may be responsible for the greater invasiveness of the Δ*SUB6* strains of *T. benhamiae* observed during RHE infection. Accordingly, the *SUB6*-deleted strain of *T. interdigitale* ATCC 28185 showed a higher proteolytic activity than the WT strain (Shi et al, 2016).

In conclusion, by comparing the development of infection in RHE between reference and Δ*SUB6* strains of *T. benhamiae* and *T. mentagrophytes*, we identified a role for SUB6 in the initial adhesion of dermatophyte spores to the host epidermis. However, owing to potential compensatory mechanisms, SUB6 alone is not an indispensable actor in the establishment of infection and therefore not a sufficient target to develop therapeutic approaches. Nevertheless, because *SUB6* expression is associated with dermatophyte infection, regardless of its possible role in the infectious process, SUB6 is a robust fungal marker of dermatophytosis that might be an interesting target for clinical diagnosis.

MATERIALS AND METHODS

Dermatophyte strains and genetic manipulation

All *T. benhamiae* and *T. mentagrophytes* strains, listed in Tables 1 and 2, were maintained on Sabouraud glucose agar (SGA) (BD Bioscience). The *T. benhamiae KU70*—lacking mutant (Tb-Δ*KU70*), which was produced from the WT strain IHEM 20161 (Figure 7), and the *T. mentagrophytes* dominant selectable marker (hygromycin B phosphotransferase gene)—free *KU80*-lacking mutant 1062Av1401 (Tm-Δ*KU80*) (Yamada et al, 2014), derived from TmKu80Δ49 (Yamada et al, 2009), were used as the recipient strains for genetic manipulation. Microconidium formation was induced at 28 °C using 1/10 SGA, supplemented with 500 μg/ml cycloheximide (Wako Chemical) and 50 μg/ml chloramphenicol (Wako Chemical). *Agrobacterium tumefaciens* EHA105 was maintained as previously

significant differences between the Δ*SUB6* strain and the other strains for each gene; Cq > 45). Complete names and accession numbers of studied genes are listed in Supplementary Tables S4 and S5. ND, nondetected; RHE, reconstructed human epidermis.

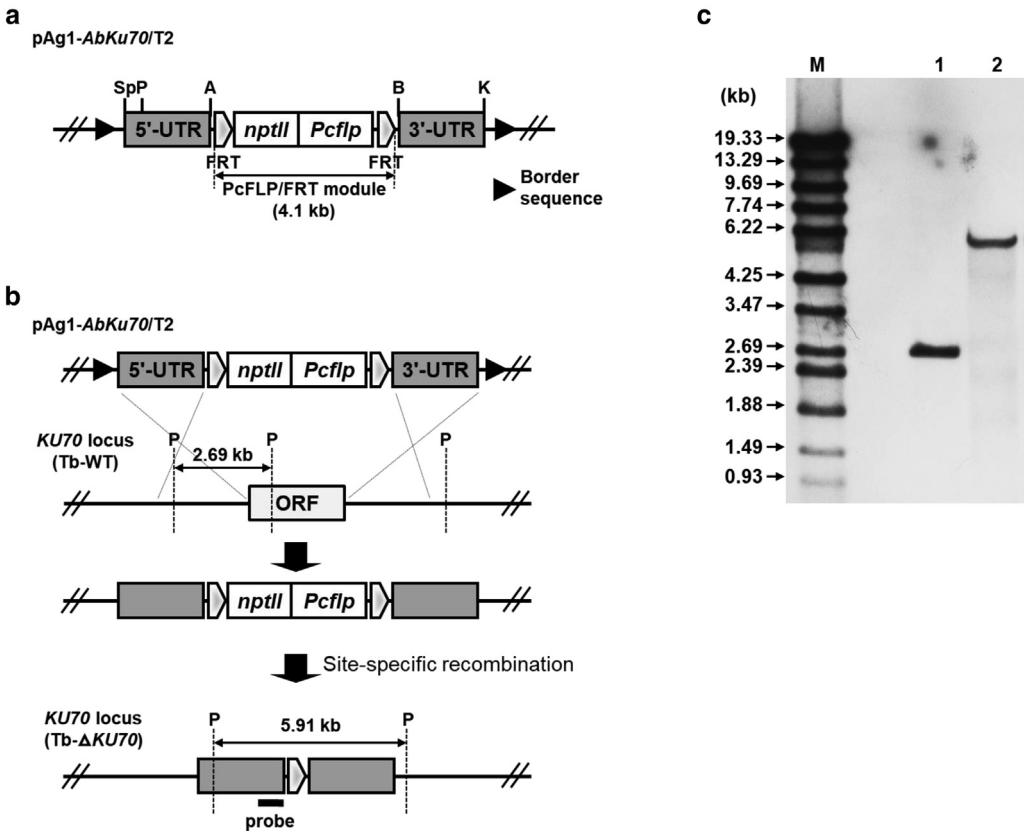

Figure 7. Production of a *Trichophyton benhamiae* mutant strain lacking the *KU70* gene (Tb-Δ*KU70*). (**a**) Schematic representation of the binary *KU70*-targeting vector pAg1-*AbKu70*/T2. The nptII cassette is composed of *Aspergillus nidulans trpC* promoter (*PtrpC*), *E. coli* neomycin phosphotransferase gene (*nptII*), and *A. fumigatus cgrA* terminator (TcgrA). Border sequences are the specific regions that delineate the DNA to be transferred during *A. tumefaciens*—mediated transformation. Restriction enzyme sites: A, ApaI; B, BamHI; K, KpnI; P, PstI; and Sp, SpeI. **(b)** Disruption of the *KU70* gene was achieved by transformation of the WT strain (Tb-WT) with the PcFLP/FRT module from the pAg1-*AbKu70*/T2 vector. The PcFLP/FRT module was then excised by site-specific recombination between the flanking FRT sequences through conditional expression of the *Pcflp* gene after transformation. **(c)** Verification of the deletion in the *KU70* locus by Southern blotting analysis. Aliquots of approximately 10 μg of genomic DNA from each strain were digested with PstI and separated by electrophoresis on 0.8% (w/v) agarose gel. Lane 1, Tb-WT (parent strain); lane 2, Tb-Δ*KU70*. A fragment of about 520 bp of the *KU70* locus was amplified by PCR with a pair of the primers P15 and P16 (Supplementary Table S1) and used as a hybridization probe. DNA standard fragment sizes are shown on the left. UTR, untranslated region; WT, wild-type.

described (Yamada et al, 2009). *E. coli* DH5α (Nippon Gene) was used for molecular cloning.

Total dna extraction. Total DNA was extracted according to the method of Girardin and Latge (1994). The growing mycelia of each dermatophyte strain were collected after incubation on SGA for 3—4 days at 28 °C, frozen in liquid nitrogen, and ground twice with a Multi-Beads shocker (Yasui Kikai) at 2000 r.p.m. for 10 seconds.

Construction of gene replacement vectors for targeted gene disruption. The *T. benhamiae SUB6*—targeting vector was constructed from the binary vector pAg1-*AbKu70*/T2 (Figure 7). The 2.00 kb of the 5′- and 3′ untranslated regions (UTRs) of the *SUB6* gene from *T. benhamiae* (ARB_05307) were amplified from total DNA of the Tb-Δ*KU70* strain by PCR with the P1—P4 and P5—P6 primer pairs, respectively (Supplementary Table S1). Each fragment was double digested with the SpeI/ApaI and the BamHI/KpnI enzymes, respectively, and inserted into the corresponding sites within pAg1-*AbKu70*/T2 to generate pAg1-*AbSUB6*/T (Figure 8 and Table 3). For complementation of *SUB6* gene in the *T. benhamiae* Δ*SUB6* strain, an approximately 3.0 kb fragment containing the 5′ UTR and the coding region of the *SUB6* gene was amplified from total DNA of the Tb-Δ*KU70* strain by PCR using the P7—P10 primers (Supplementary Table S1). The resulting fragment was digested with SpeI/ApaI and inserted into the SpeI/ApaI site of pAg1-*AbSUB6*/T to generate pAg1-*AbSUB6*/C (Figure 8 and Table 3).

The *T. mentagrophytes SUB6*—targeting vector pMRV-*AvSUB6*/T was constructed from pMRV-*TmKu80*/T2 (Figure 9 and Table 4). Approximately 2.4 kb of the 5′ and 3′ UTRs of the *SUB6* gene from *T. mentagrophytes* (AHY02992.1) were amplified from total DNA of Tm-WT strain by PCR using the following primer pairs: P17—P22 and P23—P24 (Supplementary Table S2). Each fragment was double digested with the SpeI/ApaI and the BamHI/KpnI enzymes, respectively, and inserted into the corresponding sites within pMRV-*TmKu80*/T2 to generate pMRV-*AvSUB6*/T (Figure 9 and Table 4). For complementation of *SUB6* gene in the Tm-Δ*SUB6* strain (Yamada et al, 2014), an approximately 3.08 kb fragment containing the 5′ UTR and the coding region of *SUB6* gene was amplified from total DNA of the Tm-Δ*KU80* strain by PCR with the following primer pair: P25—P28 (Supplementary Table S2). The resulting fragment was double digested with SpeI/ApaI. The 3′ UTR fragment of *SUB6* gene was excised from pMRV-*AvSUB6*/T with BamHI/KpnI. These 2 fragments were inserted into the corresponding sites of pAg1-*AbKu70*/T2, respectively, to generate pAg1-*AvSUB6*/C (Figure 9 and Table 4).

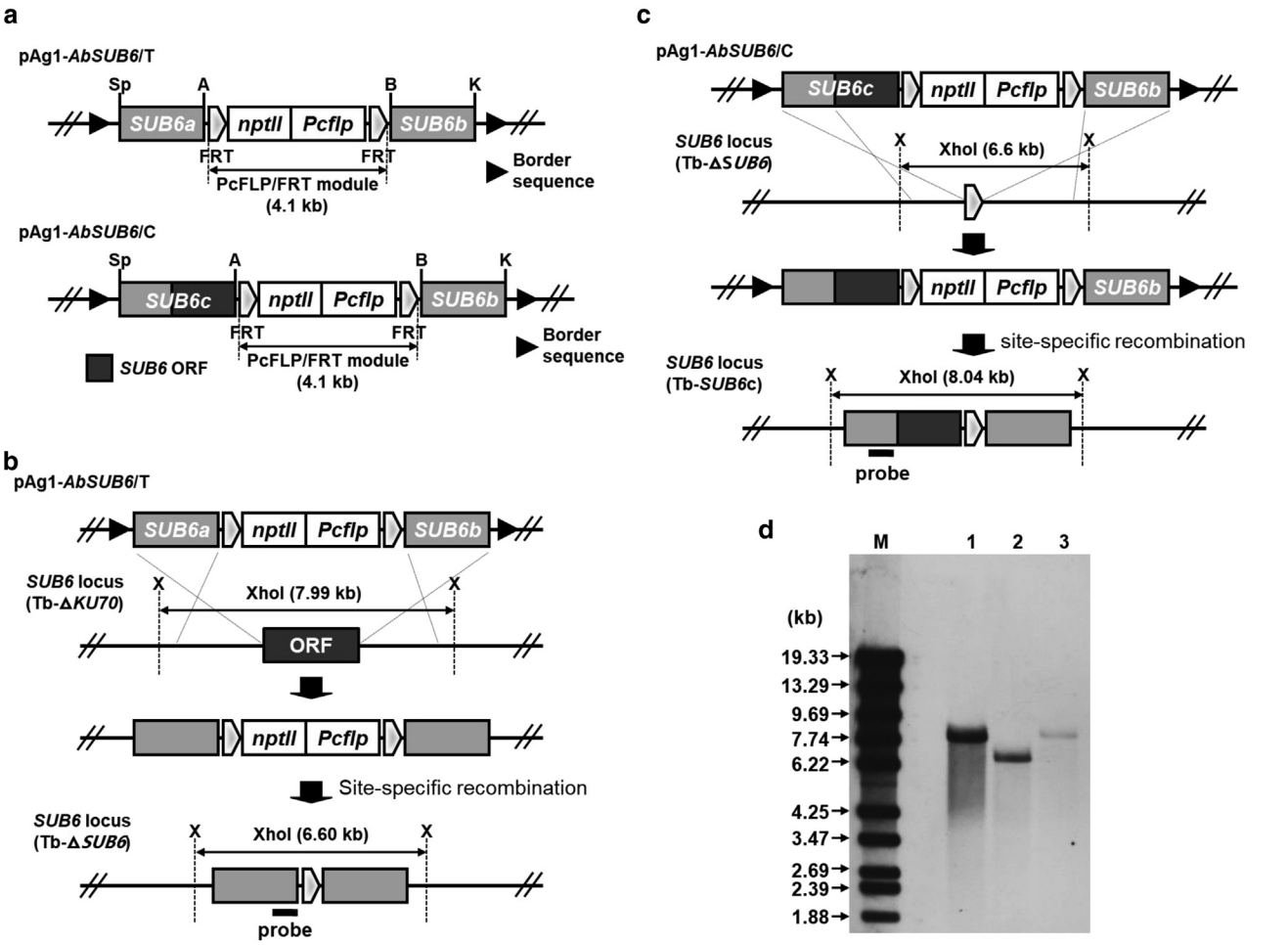

Figure 8. Disruption of the *SUB6* gene and subsequent reintroduction by a gene replacement strategy in the *Trichophyton benhamiae* Δ*KU70* strain. (**a**) Schematic representation of the binary *SUB6*-targeting vector pAg1-*AbSUB6*/T and the binary *SUB6*-complementation vector pAg1-*AbSUB6*/C. Border sequences are the specific regions that delineate the DNA to be transferred during *A. tumefaciens*–mediated transformation. Restriction enzyme sites: A, ApaI; B, BamHI; K, KpnI; Sp, SpeI; and X, XhoI. **(b)** Disruption of the *SUB6* gene was achieved by transformation of the recipient strain Tb-Δ*KU70* with the PcFLP/FRT module from the pAg1-*AbSUB6*/T vector. The PcFLP/FRT module was then excised by site-specific recombination between the flanking FRT sequences through conditional expression of the *Pcflp* gene after transformation. **(c)** Reintroduction of the *SUB6* gene by transformation of the strain Tb-Δ*SUB6* with the PcFLP/FRT module from the pAg1-*AbSUB6*/C vector. The PcFLP/FRT module was then excised by site-specific recombination between the flanking FRT sequences through conditional expression of the *Pcflp* gene after transformation. **(d)** Verification of the deletion and subsequent reintroduction in the *SUB6* locus by Southern blotting analysis. Aliquots of approximately 10 μg of genomic DNA from each strain were digested with PstI and separated by electrophoresis on 0.8% (w/v) agarose gel. Lane 1, Tb-Δ*KU70* (parent strain); lane 2, Tb-Δ*SUB6* (*SUB6*-deleted strain); and lane 3, Tb-*SUB6*c (*SUB6*-complemented strain). A fragment of about 540 bp of the *SUB6* locus was amplified by PCR with primers P15 and P16 (Supplementary Table S2) and used as a hybridization probe. DNA standard fragment sizes are shown on the left.

Table 3. Plasmids Used for Generation of *Trichophyton benhamiae*–Mutant Strains

Plasmid	Description
pAg1[1]	A streamlined version of the binary vector pBIN19 containing sequences necessary for replication in *E. coli* and *A. tumefaciens* (*oriV, trfA*), *E coli* neomycin phosphotransferase (*nptII*), and the T-DNA region. A multiple cloning site was placed within the T-DNA region.
pAg1-*AbKu70*/T2[2]	AbKu70a fragment (the 5′-UTR of *KU70* gene; 2.49kb), 5′-FLP recombination target (FRT), *PtrpC* (X02390), *nptII*, *TcgrA* (AFUA_8G02750), *Pctr4* (TERG_01401), *Penicillium chrysogenum*–optimized *Pcflp*, *Ttrp1* (M74901), 3′-FRT sequence, AbKu70b fragment (the 3′-UTR of *KU70* gene; 2.19 kb)
pAg1-*AbSUB6*/T	*SUB6*a fragment (the 5′-UTR of *SUB6* gene; 2.0 kb), 5′-FRT sequence, *PtrpC*, *nptII*, *TcgrA*, *Pctr4*, *Pcflp*, *Ttrp1*, 3′-FRT sequence, *SUB6*b fragment (the 3′-UTR of *SUB6* gene; 2.02 kb)
pAg1-*AbSUB6*/C	*SUB6*c fragment (the 5′-UTR and the coding region of *SUB6* gene; 2.95 kb), 5′-FRT sequence, *PtrpC*, *nptII*, *TcgrA*, *Pctr4*, *Pcflp*, *Ttrp1*, 3′-FRT sequence, *SUB6*b fragment (the 3′-UTR of *SUB6* gene; 2.02 kb)

Abbreviations: T-DNA, transferable DNA; UTR, untranslated region.
[1]Zhang et al (2003).
[2]Yamada et al (2017).

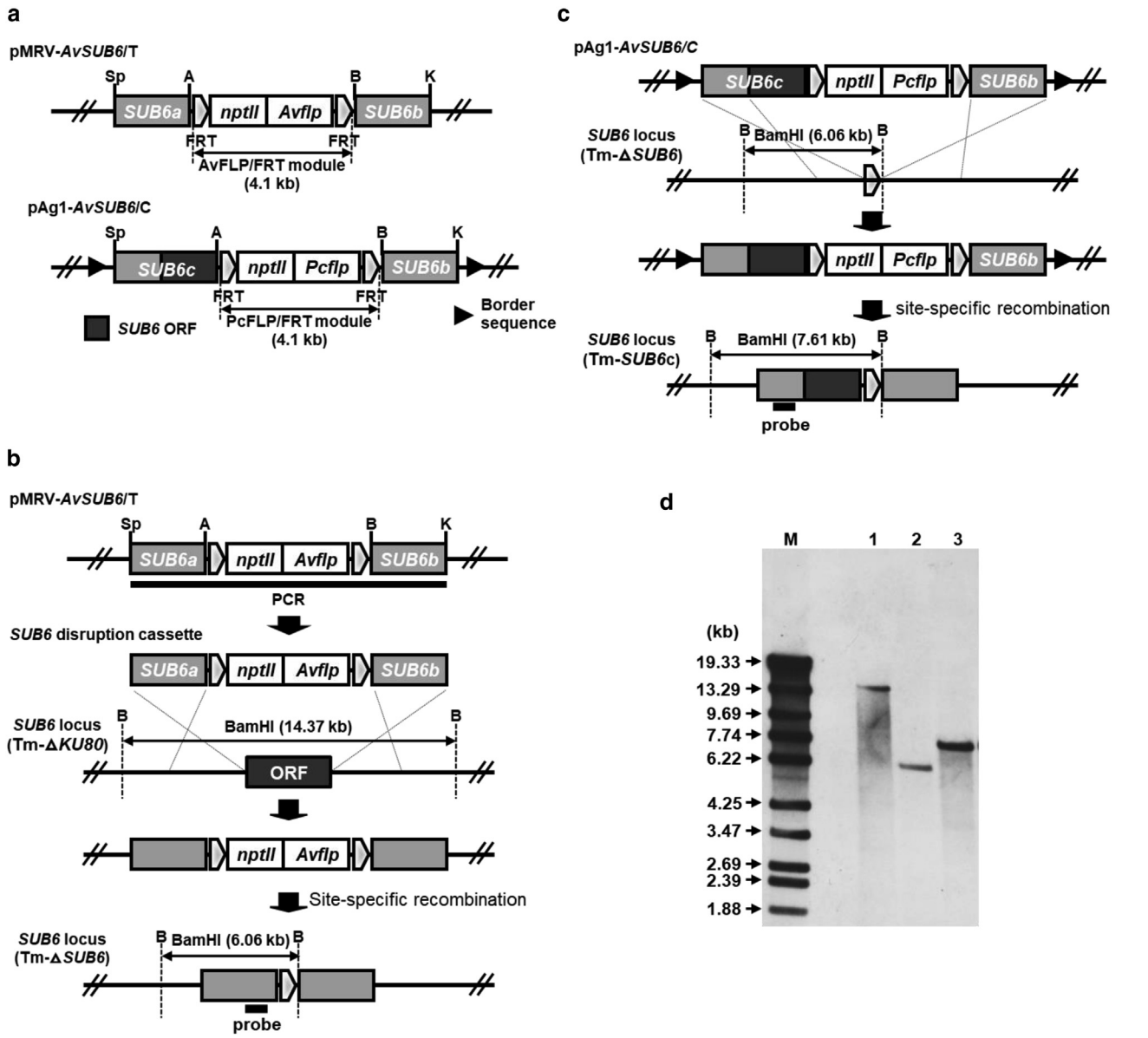

Figure 9. Disruption of the *SUB6* gene and subsequent reintroduction by a gene replacement strategy in the *Trichophyton mentagrophytes* Δ*KU80* strain. (**a**) Schematic representation of the *SUB6*-targeting vector pMRV-*AvSUB6*/T and the binary *SUB6*-complementation vector pAg1-*AvSUB6*/C. Border sequences in pAg1-*AvSUB6*/C are the specific regions that delineate the DNA to be transferred during *A. tumefaciens*—mediated transformation. Restriction enzyme sites: A, ApaI; B, BamHI; K, KpnI; and Sp, SpeI. **(b)** Disruption of the *SUB6* gene was achieved by transformation of the recipient strain Tm-Δ*KU80* with the AvFLP/FRT module from the pMRV-*AvSUB6*/T vector. The AvFLP/FRT module was then excised by site-specific recombination between the flanking FRT sequences through conditional expression of the *Avflp* gene after transformation. **(c)** Reintroduction of the *SUB6* gene by transformation of the strain Tm-Δ*SUB6* with the PcFLP/FRT module from the pAg1-*AvSUB6*/C vector. The PcFLP/FRT module was then excised by site-specific recombination between the flanking FRT sequences through conditional expression of the *Pcflp* gene after transformation. **(d)** Verification of the deletion and subsequent reintroduction in the *SUB6* locus by Southern blotting analysis. Aliquots of approximately 5 μg of genomic DNA from each strain were digested with BamHI and separated by electrophoresis on 0.8% (w/v) agarose gel. Lane 1, Tm-Δ*KU80* (parent strain); lane 2, Tm-Δ*SUB6* (*SUB6*-deleted strain); and lane 3, Tm-*SUB6*c (*SUB6*-complemented strain). A fragment of about 520 bp of the *SUB6* locus was amplified by PCR with primers P22 and P27 (Supplementary Table S2) and used as a hybridization probe. DNA standard fragment sizes are shown on the left.

All PCR reactions were performed using PrimeSTAR HS and PrimeSTAR GXL DNA polymerases or Extaq DNA polymerase (Takara Bio). If necessary, the internal ApaI, BamHI, KpnI, and SpeI sites contained in the amplified fragments were inactivated by overlap extension PCR using appropriate primer pairs. The nucleotide sequences of all the primers used are listed in Supplementary Tables S1 and S2. If necessary, the amplified fragments were gel purified with a QIAEX II gel extraction kit (Qiagen), subcloned into HincII-digested pUC118, and sequenced.

Fungal genetic transformation. Genetic transformation of each *T. benhamiae* strain was performed according to the previously described *A. tumefaciens*—mediated transformation method (Yamada et al, 2017). After cocultivation, nylon membranes were

Table 4. Plasmids Used for Generation of *Trichophyton mentagrophytes*—Mutant Strains

Plasmid	Description
pMRV-*TmKu80*/T2[1]	*TmKu80* gene fragment (AB427108) (position −66 to 1444, 1.51 kb), 5′-FRT sequence, *PtrpC*, *nptII*, *TcgrA*, *Pctr4*, *T. mentagrophytes*—optimized *flp* gene (*Avflp*), *Ttrp1*, 3′-FRT sequence, *TmKu80* gene fragment (positions 1533−3054, 1.52 kb)
pMRV-*AvSUB6*/T[1]	SUB6a fragment (the 5′-UTR of *SUB6* gene, 2.36 kb), 5′-FRT sequence, *PtrpC*, *nptII*, *TcgrA*, *Pctr4*, *avflp*, *Ttrp1*, SUB6b fragment (the 3′-UTR of *SUB6* gene, 2.45 kb)
pAg1-*AvSUB6/C*	SUB6c fragment (the 5′-UTR and the coding region of *SUB6* gene, 3.08 kb), 5′-FRT sequence, *PtrpC*, *nptII*, *TcgrA*, *Pctr4*, *Pcflp*, *Ttrp1*, 3′-FRT sequence, SUB6b fragment

Abbreviation: UTR, untranslated region.
[1]Yamada et al (2014).

transferred onto SGA containing 250 μg/ml G418 (Wako) and 10 μM copper(II) sulphate pentahydrate and overlaid with 10 ml of the same solution. After 48 hours, the plates were further overlaid with 10 ml of SGA containing 350 μg/ml G418 and 10 μM copper(II) sulphate pentahydrate and incubated for 4−5 days. Colonies regenerating on the selective media were considered as putative G418-resistant clones and were transferred onto MOPS-buffered RPMI 1640A agar medium supplemented with 500 μg/ml cycloheximide, 50 μg/ml chloramphenicol, 200 μg/ml cefotaxime sodium (Sanofi-Aventis), and 20 μM bathocuproine disulfonate (Dojindo Laboratories) and passaged several times. The *T. rubrum* ctr4 promoter (*Pctr4*) is a conditional promoter that is repressed in the presence of copper. Chelation of copper by bathocuproine sulfate activates the Pctr4, leading to the induction of the *Pcflp* gene expression. Expression of PcFLP recombinase leads to excision of the selectable marker through PcFLP-mediated site-specific recombination between the flanking FRT sequences.

Genetic transformation of the *T. mentagrophytes* Δ*KU80* strain for *SUB6* gene deletion was performed by the protoplast/polyethylene glycol−mediated method as previously described (Yamada et al, 2014). Colonies regenerating on the selective medium (SGA containing 250 μg/ml G418 and 10 μM copper(II) sulphate pentahydrate) were picked up as putative G418-resistant clones, transferred onto RPMI1640A medium, and passaged multiple times to activate the Pctr4, leading to the induction of the *Avflp* gene expression and subsequent excision of the selectable marker through AvFLP-mediated site-specific recombination between the flanking FRT sequences. Complementation of the *SUB6* gene in the Δ*SUB6* strain was performed by the *A. tumefaciens*−mediated transformation method as described earlier.

Screening of the desired transformants. The desired transformants were finally screened by PCR, Southern blot analysis, and nucleotide sequencing. Aliquots of 50−100 ng of the total DNA were used as templates in the PCR reactions. For Southern blot analysis, aliquots of approximately 5−10 μg of the total DNA were digested with an appropriate restriction enzyme, separated by electrophoresis on 0.8% (w/v) agarose gels, and transferred to Hybond-N+ membranes (Cytiva). Southern hybridization was performed using the ECL Direct Nucleic Acid Labelling and Detection System (Cytiva), according to the manufacturer's instructions.

Production of fungal suspension for RHE infection

All strains of *T. benhamiae* and *T. mentagrophytes* (Tables 1 and 2) were grown on SGA at 30 °C, and then the spore suspensions were prepared following a recently published method by Faway et al (2021a). Briefly, after growth on SGA, dermatophyte sporulation was induced by incubation on potato dextrose agar at 30 °C and under 12% carbon dioxide. The fungal material was harvested and filtered through Miracloth layers (Millipore), and the unicellular spores were finally suspended in PBS. The resulting spore suspensions are composed of microconidia and enriched in arthroconidia, whose percentage reaches up to 21 and 9% for *T. benhamiae* IHEM 20161 and *T. mentagrophytes* TIMM 2789, respectively (Faway et al, 2021a). For simplicity, microconidia and arthroconidia are collectively referred to as "spores" throughout this paper. The total concentration of spores in the resulting suspension was determined by counting colony-forming units after 3 days of incubation on SGA at 30 °C.

Infection model on RHE

RHE was prepared from normal human keratinocytes (Human Epidermal Keratinocytes, adult; Thermo Fisher Scientific) on 0.6 cm^2 polycarbonate filter inserts (Merck), following a previously published procedure (De Vuyst et al, 2014).

RHE was infected by topical application of spore suspension as previously described by Faway et al (2017). The fungal load in the inoculum was adjusted to 30 colony-forming units for *T. benhamiae* and 150 colony-forming units for *T. mentagrophytes*, as previously determined to induce fungal invasion of the epidermis limited to the cornified layer on day 3 or 4 after infection, respectively (Faway et al, 2025) (Figures 1 and 2). Four hours after inoculation, PBS washes were performed to remove nonadherent spores and re-expose RHE to air. Infected RHE was then maintained in culture until day 3 or 4 after infection and finally harvested for histological analysis and total RNA extraction (late infection).

The integrity of the epidermal barrier was monitored during infection by measuring the TEER across the RHE using a Millicell ERS-2 Voltohmmeter (Millipore). These measurements are expressed as a percentage of the TEER values measured across the RHE before infection.

To assess spore adhesion to the epidermal surface, nonadherent spores recovered during PBS washes, performed after 30 minutes, 1 hour, 2 hours, or 4 hours of contact were counted on SGA to determine the percentage of remaining adherent spores, as previously done (Faway et al, 2017).

To study fungal gene expression during early infection, an inoculum of 1.10^8 colony-forming units was applied topically onto RHE. After 30 minutes of contact, allowing for reactivation of the spores upon contact with the epidermal tissue, activated spores were collected by washing with PBS and centrifuged for RNA extraction from the spore pellet.

Histological analysis

Infected RHE was fixed in a 4% formaldehyde solution and histologically processed as previously described (Faway et al, 2017).

Periodic-acid Schiff staining with α-amylase pretreatment and hemalun counterstaining was performed to highlight fungal elements. When observing the slides under the microscope (Olympus), the area stained by periodic-acid Schiff could be quantified, giving a value for the extent of the invasion.

RNA extraction and RT-qPCR

Total RNA was extracted from infected RHE and reverse transcribed into cDNA according to a previously optimized procedure (Faway et al, 2025). After qPCR using Takyon NO ROX SYBR Master Mix (Eurogentec) and specific primers listed in Supplementary Tables S3–5, the relative expression of human and fungal genes was calculated using the $2^{-\Delta\Delta Cq}$ method, using human *RPLP0* and fungal *βTUB* as reference genes. Because the fungal expression profile differs according to phenotype (spores or hyphae), adequate control samples must be used to analyze gene expression levels in dermatophytes during early and late infection in RHE. As previously done (Faway et al, 2025), RNA extracted from a pellet of spores and from fungal mycelium, recovered after 24 hours of growth in Sabouraud glucose broth, was used as relativization control for early and late infection, respectively.

Statistical analyses

For each experiment in RHE, 3 independent experimental replicates were performed using freshly prepared RHE and spore suspensions. For RNA expression measurements, 2 technical replicates were performed for each experimental replicate; practically, for each experimental replicate, 2 RHEs were identically treated and processed before RNA was extracted from both and pooled before being subjected to RT-qPCR.

All statistical analyses were performed with SigmaPlot, version 11.0 (Systat Software). Shapiro–Wilk normality test followed by 1-way or 2-way ANOVA was carried out, and a $P \leq .05$ was considered statistically significant. Two-way repeated-measures ANOVA was used for statistical analysis of the TEER experiments, which allowed monitoring of the same RHE over time.

ETHICS STATEMENT

This paper does not report human or animal studies. Normal human keratinocytes used for the production of reconstructed human epidermis were purchased from Thermo Fisher Scientific (Human Epidermal Keratinocytes, adult).

DATA AVAILABILITY STATEMENT

No large datasets were generated or analyzed during this study. The data that support the findings of this study are available from the corresponding author (emilie.faway@unamur.be) upon request.

CONFLICT OF INTEREST

The authors state no conflict of interest.

ORCIDs

Émilie Faway: http://orcid.org/0000-0003-3406-1103
Wilfried Poirier: http://orcid.org/0000-0002-2687-3032
Tsuyoshi Yamada: http://orcid.org/0000-0002-1394-5455
Kiyotaka Ozawa: http://orcid.org/0009-0004-2810-9443
Michel Monod: http://orcid.org/0000-0002-0695-4003
Bernard Mignon: http://orcid.org/0000-0002-5958-4325
Yves Poumay: http://orcid.org/0000-0001-5200-3367

ACKNOWLEDGMENTS

The authors gratefully acknowledge the technical help provided by V. Bielarz, V. De Glas, and K. De Swert. This work was supported by the Région Wallonne and StratiCELL (MYCEPI, grant number 1910074) and by the Ministry of Education, Culture, Sports, Science and Technology of Japan through a Grant-in-Aid for Scientific Research (C) (20K07054).

AUTHOR CONTRIBUTIONS

Conceptualization: EF, WP, TY, MM, BM, YP; Data Curation: EF, TY; Formal Analysis: EF; Funding Acquisition: EF, TY, BM, YP; Investigation: EF, TY, KO; Methodology: EF, WP, TY, MM, BM, YP; Project Administration: EF; Supervision: EF, WP, TY, MM, BM, YP; Validation: EF, WP, TY, MM, BM, YP; Visualization: EF; Writing – Original Draft Preparation: EF, WP, TY, MM, BM, YP; Writing – Review and Editing: EF, WP, TY, MM, BM, YP

DECLARATION OF GENERATIVE ARTIFICIAL INTELLIGENCE (AI) OR LARGE LANGUAGE MODELS (LLMs)

The author(s) did not use AI/LLM in any part of the research process and/or manuscript preparation.

SUPPLEMENTARY MATERIAL

Supplementary material is linked to the online version of the paper at www.jidonline.org, and at https://doi.org/10.1016/j.jid.2025.100370.

REFERENCES

Aho-Laukkanen E, Mäki-Koivisto V, Torvikoski J, Sinikumpu SP, Huilaja L, Junttila IS. PCR enables rapid detection of dermatophytes in practice. Microbiol Spectr 2024;12:e0104924.

Băguţ ET, Baldo A, Mathy A, Cambier L, Antoine N, Cozma V, et al. Subtilisin Sub3 is involved in adherence of Microsporum canis to human and animal epidermis. Vet Microbiol 2012;160:413–9.

Baldo A, Mathy A, Tabart J, Camponova P, Vermout S, Massart L, et al. Secreted subtilisin Sub3 from Microsporum canis is required for adherence to but not for invasion of the epidermis. Br J Dermatol 2010;162:990–7.

Baldo A, Tabart J, Vermout S, Mathy A, Collard A, Losson B, et al. Secreted subtilisins of Microsporum canis are involved in adherence of arthroconidia to feline corneocytes. J Med Microbiol 2008;57:1152–6.

Baumbach CM, Michler JK, Nenoff P, Uhrlaß S, Schrödl W. Visualising virulence factors: trichophyton benhamiaes subtilisins demonstrated in a guinea pig skin ex vivo model. Mycoses 2020;63:970–8.

De Vuyst E, Charlier C, Giltaire S, De Glas V, de Rouvroit CL, Poumay Y. Reconstruction of normal and pathological human epidermis on polycarbonate filter. Methods Mol Biol 2014;1195:191–201.

Faway E, Cambier L, De Vuyst E, Evrard C, Thiry M, Lambert de Rouvroit C, et al. Responses of reconstructed human epidermis to Trichophyton rubrum infection and impairment of infection by the inhibitor PD169316. J Invest Dermatol 2019;139:2080–9.e6.

Faway É, Cambier L, Mignon B, Poumay Y, Lambert de Rouvroit C. Modeling dermatophytosis in reconstructed human epidermis: a new tool to study infection mechanisms and to test antifungal agents. Med Mycol 2017;55:485–94.

Faway E, Poirier W, Maréchal F, Poumay Y, Mignon B. Expression of fungal and host markers in models of dermatophytosis on mice and human epidermis. J Invest Dermatol 2025;145:897–907.e8.

Faway E, Staerck C, Danzelle C, Vroomen S, Courtain C, Mignon B, et al. Towards a standardized procedure for the production of infective spores to study the pathogenesis of dermatophytosis. J Fungi (Basel) 2021a;7:1029.

Faway E, Thiry M, Mignon B, Poumay Y. Experimental models of dermatophytosis. In: Bouchara JP, Nenoff P, Gupta AK, Chaturvedi V, editors. Dermatophytes and dermatophytoses. Cham: Springer; 2021b. p. 135–60.

Girardin H, Latge J. DNA extraction and quantification. In: Maresca B, Kobayashi GS, editors. Molecular biology of pathogenic fungi. 2nd ed. New York: Telos Press; 1994. p. 5–9.

Gräser Y, Monod M, Bouchara JP, Dukik K, Nenoff P, Kargl A, et al. New insights in dermatophyte research. Med Mycol 2018;56:2–9.

Gupta AK, Wang T, Mann A, Polla Ravi S, Talukder M, Lincoln SA, et al. Antifungal resistance in dermatophytes - review of the epidemiology, diagnostic challenges and treatment strategies for managing trichophyton indotineae infections. Expert Rev Anti Infect Ther 2024;22:739–51.

Havlickova B, Czaika VA, Friedrich M. Epidemiological trends in skin mycoses worldwide [published correction appears in Mycoses 2009;52:95]. Mycoses 2008;51:2–15.

Ilkit M, Demirhindi H. Asymptomatic dermatophyte scalp carriage: laboratory diagnosis, epidemiology and management. Mycopathologia 2008;165:61–71.

Ishii M, Matsumoto Y, Yamada T, Uga H, Katada T, Ohata S. TrCla4 promotes actin polymerization at the hyphal tip and mycelial growth in Trichophyton rubrum. Microbiol Spectr 2023;11:e0292323.

Lindenhahn J, Bartosch T, Baumbach CM, Suchowski M, Kacza J, Schrödl W, et al. Detection of subtilisin 3 and 6 in skin biopsies of cattle with clinically manifested bovine ringworm. Med Mycol 2021;59:305–8.

Méhul B, Gu Z, Jomard A, Laffet G, Feuilhade M, Monod M. Sub6 (Tri r 2), an onychomycosis marker revealed by proteomics analysis of Trichophyton rubrum secreted proteins in patient nail samples. J Invest Dermatol 2016;136:331–3.

Monod M. Secreted proteases from dermatophytes. Mycopathologia 2008;166:285–94.

Monod M, Blanchard G, Guenova E. Antifungal resistance on the rise. J Invest Dermatol 2023;143:2332–4.

Poirier W, Faway É, Yamada T, Ozawa K, Maréchal F, Monod M, et al. Subtilisin 6 from the dermatophyte Trichophyton benhamiae is a marker of infection but not a unique virulence factor. Mycoses 2025;68:e70037.

Sacheli R, Hayette MP. Antifungal resistance in dermatophytes: genetic considerations, clinical presentations and alternative therapies. J Fungi (Basel) 2021;7:983.

Satala D, Bras G, Kozik A, Rapala-Kozik M, Karkowska-Kuleta J. More than just protein degradation: the regulatory roles and moonlighting functions of extracellular proteases produced by fungi pathogenic for humans. J Fungi (Basel) 2023;9:121.

Shi Y, Niu Q, Yu X, Jia X, Wang J, Lin D, et al. Assessment of the function of SUB6 in the pathogenic dermatophyte Trichophyton mentagrophytes. Med Mycol 2016;54:59–71.

Staib P, Zaugg C, Mignon B, Weber J, Grumbt M, Pradervand S, et al. Differential gene expression in the pathogenic dermatophyte arthroderma benhamiae in vitro versus during infection. Microbiology (Reading) 2010;156:884–95.

Suh SO, Grosso KM, Carrion ME. Multilocus phylogeny of the Trichophyton mentagrophytes species complex and the application of matrix-assisted laser desorption/ionization-time-of-flight (MALDI-TOF) mass spectrometry for the rapid identification of dermatophytes. Mycologia 2018;110:118–30.

Tirtiaux B, Ianiri G, De Glas V, Denil E, Faway E, Poumay Y. Invasion of human epidermis by Malassezia furfur is strain dependent. J Invest Dermatol 2025;145:696–9.e8.

Tran VD, De Coi N, Feuermann M, Schmid-Siegert E, Băguț ET, Mignon B, et al. RNA sequencing-based genome reannotation of the dermatophyte arthroderma benhamiae and characterization of its secretome and whole gene expression profile during infection. mSystems 2016;1:e00036-16.

Uchida K, Tanaka T, Yamaguchi H. Achievement of complete mycological cure by topical antifungal agent NND-502 in guinea pig model of tinea pedis. Microbiol Immunol 2003;47:143–6.

Upadhyay SK, Gautam P, Pandit H, Singh Y, Basir SF, Madan T. Identification of fibrinogen-binding proteins of Aspergillus fumigatus using proteomic approach. Mycopathologia 2012;173:73–82.

Verma SB, Panda S, Nenoff P, Singal A, Rudramurthy SM, Uhrlass S, et al. The unprecedented epidemic-like scenario of dermatophytosis in India: I. Epidemiology, risk factors and clinical features. Indian J Dermatol Venereol Leprol 2021;87:154–75.

Vermout S, Tabart J, Baldo A, Mathy A, Losson B, Mignon B. Pathogenesis of dermatophytosis. Mycopathologia 2008;166:267–75.

Woodfolk JA, Wheatley LM, Piyasena RV, Benjamin DC, PLatts-Mills TA. Trichophyton antigens associated with IgE antibodies and delayed type hypersensitivity. Sequence homology to two families of serine proteinases. J Biol Chem 1998;273:29489–96.

Yamada T, Maeda M, Alshahni MM, Tanaka R, Yaguchi T, Bontems O, et al. Terbinafine resistance of Trichophyton clinical isolates caused by specific point mutations in the squalene epoxidase gene. Antimicrob Agents Chemother 2017;61:e00115–7.

Yamada T, Makimura K, Satoh K, Umeda Y, Ishihara Y, Abe S. Agrobacterium tumefaciens-mediated transformation of the dermatophyte, Trichophyton mentagrophytes: an efficient tool for gene transfer. Med Mycol 2009;47:485–94.

Yamada T, Yaguchi T, Salamin K, Guenova E, Feuermann M, Monod M. MFS1, a pleiotropic transporter in dermatophytes that plays a key role in their intrinsic resistance to chloramphenicol and fluconazole. J Fungi (Basel) 2021;7:542.

Yamada Y, Maeda M, Alshahni MM, Monod M, Staib P, Yamada T. Flippase (FLP) recombinase-mediated marker recycling in the dermatophyte Arthroderma vanbreuseghemii. Microbiology (Reading) 2014;160:2122–35.

Zhan P, Liu W. The changing face of dermatophytic infections worldwide. Mycopathologia 2017;182:77–86.

Zhang A, Lu P, Dahl-Roshak AM, Paress PS, Kennedy S, Tkacz JS, et al. Efficient disruption of a polyketide synthase gene (pks1) required for melanin synthesis through Agrobacterium-mediated transformation of Glarea lozoyensis. Mol Genet Genomics 2003;268:645–55.